Design of two-band 150-220 GHz superconducting bolometric detection structure

D. Rauly, A. Monfardini, A.E Sanchez Colin, P. Febvre

Design of Two-band 150–220 GHz Superconducting Bolometric Detection Structure

D. Rauly[1], **A. Monfardini**[2], **A. Colin**[3], **and P. Febvre**[1]

[1]IMEP-LAHC, UMR 5130 CNRS/INPG/UJF/USAVOIE
MINATEC, Grenoble and Le Bourget du Lac, France
[2]Institut Néel, CNRS/UJF dept MCBT, Grenoble, France
[3]Instituto de Fisica de Cantabria (CSIC-UC), Santander, Spain

Abstract— We propose a pixel design, aimed to be included in an array, receiving and detecting simultaneously two bands of the Cosmic Microwave Background (CMB). It is composed of a bowtie antenna, feeding a diplexer structure to separate the signal towards two bolometric detectors at 150 and 220 GHz. The diplexer makes use of differential transmission lines of Coplanar Striplines (CPS) and Broadside Coupled Lines (BCL) types, for filtering and separation purposes. The antenna and diplexer are planned to be fabricated in a superconductive niobium thin film deposited on a Silicon substrate, while NbSi bolometers will lie on a SiN membrane. The device has been simulated by means of ADS (Agilent), CST Microwave Studio and HFSS (Ansoft) softwares. Final dimensions that take into account the kinetic inductance of the superconducting lines are proposed. Promising computation results are found, with signal separation up to 20 dB.

1. INTRODUCTION

Nowadays, a large number of astrophysical studies based on CMB observation require multi-band measurements. As an example, the detection of clusters of remote galaxies can be performed by comparing CMB photon fluxes at 150 and 220 GHz, using the model of spectral deformation of the Planck law, due to the Sunayev-Zeldovich (SZ) effect [1].

This requirement can be met by means of optical filtering, defining appropriate photometric bands, but it generally consumes a higher surface of the available focal plane. Multi-frequency detector arrays, using antenna-coupled bolometers associated with filtering functions may overcome this problem. These functions are classically achieved by millimeter circuits composed of planar transmission lines. Several designs, based on microstrip lines, have been proposed in the past [2, 3].

Microstrip transmission lines are often used coupled with slot antennas [4]. However, when an antenna of differential type is used, like a bow-tie antenna, a balun must be inserted between the feeding microstrip line and the antenna, in order to keep the symmetry of the currents repartition in the structure and not to affect the radiation pattern.

The design presented in this paper (see Fig. 5) proposes a bow-tie antenna coupled to a diplexer circuit exclusively composed of balanced differential transmission lines, thus avoiding the need for a balun. The strategy for elaborating the whole diplexer structure, consists of utilizing high-impedance CPS lines connected on one end to the source antenna, and to the other end to the low-impedance BCLs. The BCLs are connected to the resistive bolometers on their other end (see Fig. 5). CPS lines facilitate the decoupling between both 150 and 220 GHz sub-circuits, while BCLs lower the influence of the membrane supporting the loads and the bolometers.

2. ANTENNA DESIGN

The antenna is a bow-tie fabricated with superconductive Nb on 30 µm-thick Si substrate, with a reflector back plane located 300 µm below the antenna plane. The two triangles of the antenna (height 580 µm and base 580 µm) are separated by a 2 µm gap. Fig. 1 shows other geometric parameters for the computation. The metallization has been assumed to be 1 µm-thick perfect conductor material. Open radiation type boundaries have been defined for the surrounding box.

Figure 2 compares results computed by HFSS (Ansoft) and CST Microwave Studio softwares, in terms of real and imaginary part of the antenna impedance, seen from the 2-µm gap.

It exhibits an out-of band resonance at 100 GHz, found somewhat sharper with CST than with HFSS. Both results show good fit for the impedance values $Z_{ant} = 54.2 - j84.0\,[\Omega]$ at 150 GHz and $Z_{ant} = 108.7 + j8.5\,[\Omega]$ at 220 GHz. Consequently, the diplexer structure studied in the next

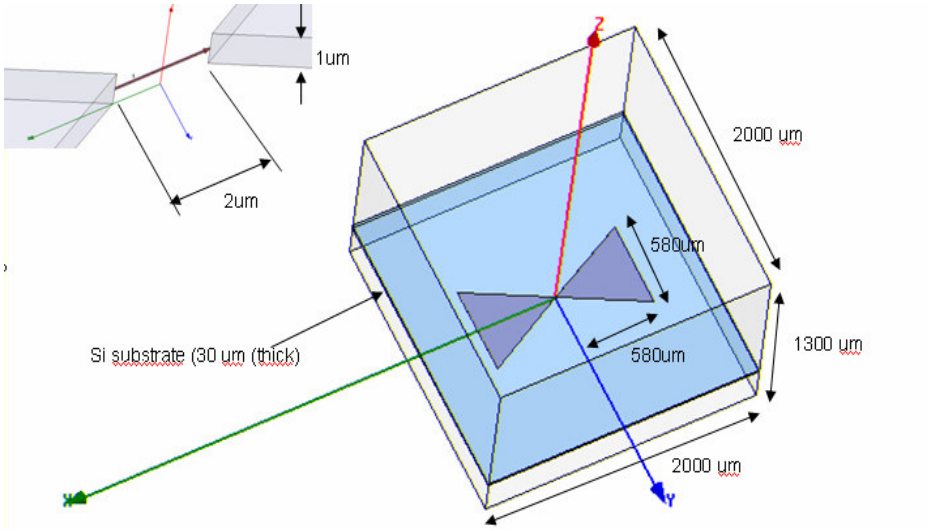

Figure 1: Geometry of the bow-tie antenna with HFSS-CST computation parameters.

paragraph must be designed in order to deliver the complex conjugate of the antenna impedance, for optimal microwave power matching.

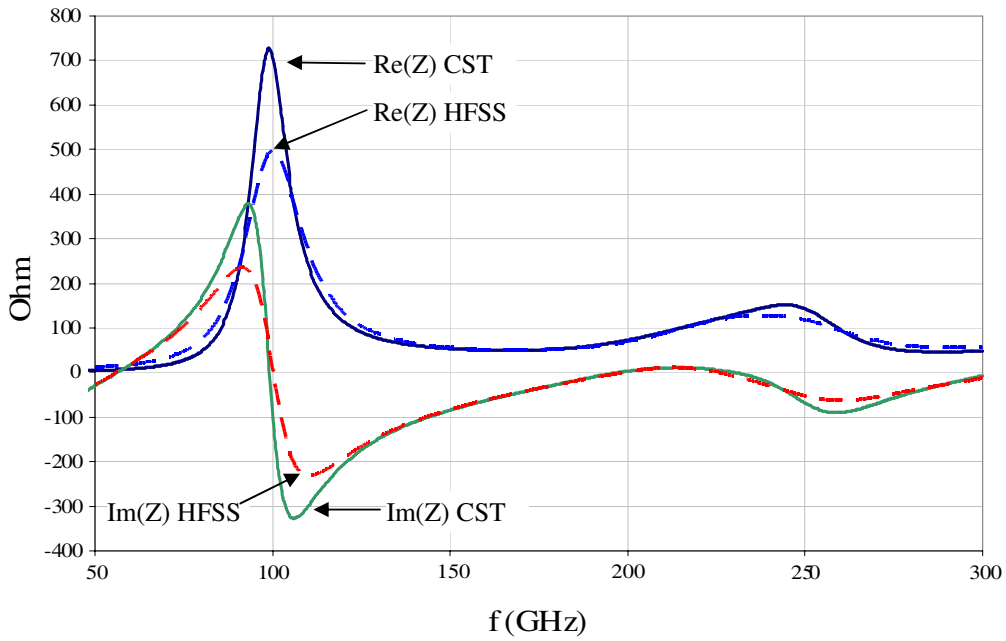

Figure 2: HFSS and CST computed antenna complex impedance.

3. DIPLEXER DESIGN

The diplexer is designed according to the simple scheme shown in Fig. 3. At this step of the project development, no severe slope has been specified for the transmission coefficient versus frequency variation. Focus is put on low insertion losses at the desired frequency, and high rejection at the undesired frequency. In this approach, each filtering sub-circuit is thus composed by only two transmission line elements, in order to meet the low-size requirement for the whole device.

In Fig. 3, Port 1 represents the antenna, modeled by its complex impedance imported from HFSS and CST computations (see Fig. 2), while Ports 2 and 3 represent the resistive loads associated to the bolometric detection. ADS Optimization has been performed with 0-dB-goals for S_{21} and S_{31} at 150 and 220 GHz respectively.

Optimized values of the characteristics impedance and electrical lengths (degrees) of the lines

are given in Fig. 3. The corresponding results are plotted in Fig. 4, in terms of reflection and transmission coefficients. It exhibits return losses and signal separation better than 20 dB, with 0 dB insertion losses at the central frequencies. Undesirable transmissions occur at 110 and 290 GHz towards the 220-GHz and 150-GHz detectors respectively, but they can be filtered, by means of a 120–240 GHz optical filter using combined metal cross-mesh and low-pass.

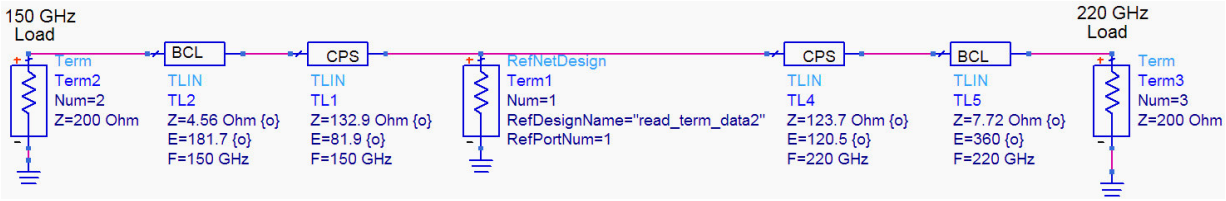

Figure 3: Schematics of the diplexer.

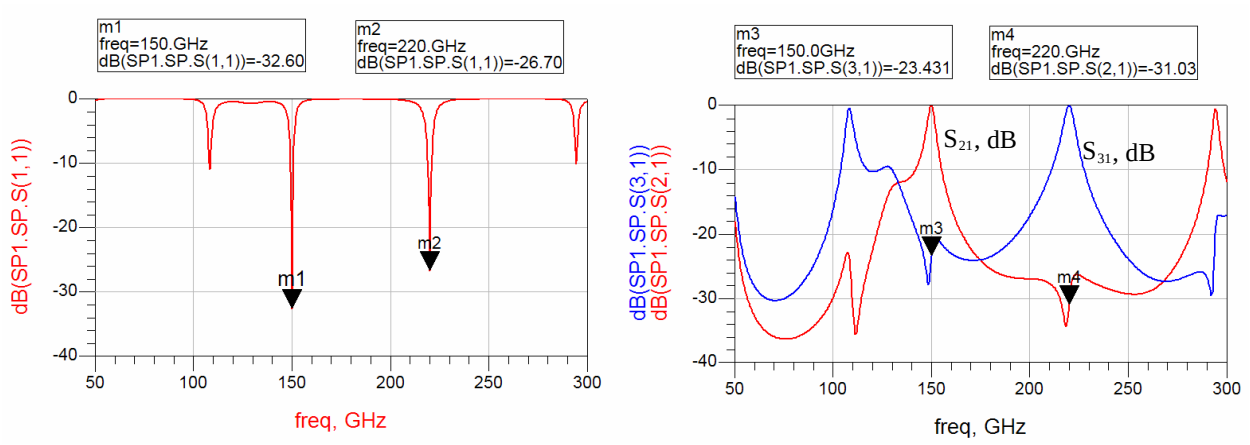

Figure 4: (a) Reflection coefficient of the structure, seen from the antenna port. (b) Transmission coefficients from antenna to 150-GHz load (S_{21} dB) & 220-GHz load (S_{31} dB).

4. LAYOUT AND PHYSICAL DIMENSIONS

The whole device is represented in Fig. 5. Notice that the strips in CPS lines TL1 and TL4 are vertically offseted by a 0.3 µm SiO_2 layer in order to permit the transition to the BCLs.

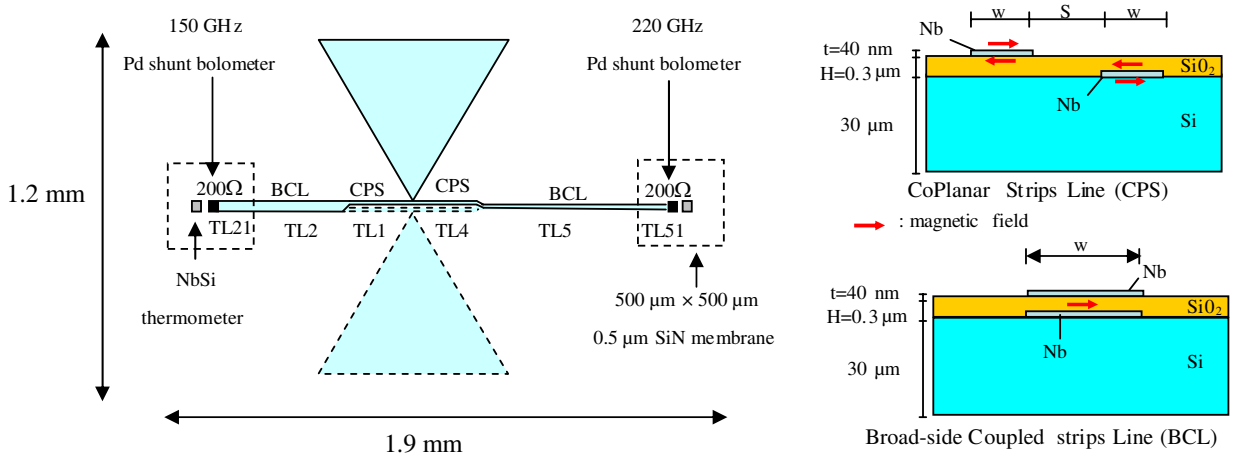

Figure 5: Left: Layout of one pixel of the detector structure. Right: Cross-section of CPS lines and BCLs.

Physical dimensions of the transmission lines have been determined using an iterative procedure. In a first step, geometrical (or external) line inductance L_{geo} and capacitance C have been deduced

from CST simulations assuming perfect conductor materials, as shown in Table 1. Next, the kinetic inductance, inherent to the superconducting state of niobium material at 0.1 K is evaluated as follows [5].

Table 1: Final dimensions of the structure and calculations of lines parameters with $\lambda_L = 39\,\text{nm}$.

TL	Phys. dim. µm	Z_c,, Ω, CST (perf. cond)	ε_{eff}, CST (perf. cond.)	L_{geo}, nH/m	C, pF/m	2*L_{kin} nH/m	Z_{superc}, Ω (eq.3)	Z_{superc}, Ω HFSS	Zc, Ω required
TL1: CPS	W=3.6 µm S=10 µm L = 186 µm	129.9	5.8	1042	61.7	28.8	**131.7**	**133.1**	132.9
TL2: BCL	W=14 µm H=0.3 µm L = 441 µm	3.9	3.8	25	1693	9.1	**4.5**	**4.8**	4.6
TL4: CPS	W= 4.5 µm S=10 µm L = 186 µm	122.5	5.80	988	65.9	23.1	**123.9**	**127**	123.7
TL5: BCL	W=8 µm H=0.3 µm L = 597 µm	6.6	3.8	43	978	16	**7.8**	**8.3 (Si) 7.8 (memb)**	7.7

For the BCLs, we assumed that the magnetic field is confined between strips, without variation in the transverse direction (horizontal in Fig. 5) due to the high aspect ratio of the BCLs. Thickness t is taken into account since it is of the same order of magnitude as the London penetration depth ($\lambda_L = 39\,\text{nm}$ for bulk Nb), and the commonly adopted assumption $t \gg \lambda_L$ is no more applicable here. As the temperature 0.1 K is far from the critical temperature of Nb 9.2 K, the electrical conductivity σ is assumed purely imaginary [6]. The kinetic inductance can be written as follows, where W is the strip width [5]:

$$L_{kin-\text{BCL}} = \mu_0 \frac{\lambda_L}{W} \coth\left(\frac{t}{\lambda_L}\right) \text{[H/m]} \tag{1}$$

For the CPS lines, attention must be paid to the magnetic field repartition, which can be considered equal, but of opposite signs, on upper and lower surfaces of the strip (see Fig. 1). The kinetic inductance then becomes [5]:

$$L_{kin-\text{CPS}} = \mu_0 \frac{\lambda_L}{2W} \coth\left(\frac{t}{2\lambda_L}\right) \text{[H/m]} \tag{2}$$

Then, assuming that all superconducting films have the same London penetration depth and thickness t, the final expression of the characteristic impedance Z_{superc} and electrical length E are:

$$Z_{superc} = \sqrt{\frac{L_{geo} + 2L_{kin}}{C}} \tag{3}$$

$$E = 360\sqrt{(L_{geo} + 2L_{kin})C} \cdot F \cdot P \text{ [degrees]} \tag{4}$$

where F is the frequency and P the physical length. Table 1 gives the calculations and final dimensions of the lines composing the diplexer. An imposed part (250 µm) of BCLs lines length is lying on the SiN membrane, but negligible correction (2%) of the strip width has been found in order to keep constant the characteristic impedance and the effective permittivity.

These results are then compared with HFSS computations where the superconductive strips are replaced by a boundary surface with purely reactive surface impedance as in reference [5]. Low dispersive effects have been found (Z_c varies less than 0.5%) but greater influence of the membrane on BCLs is revealed (see Table 1).

5. CONCLUSIONS

The design of a two band 150–220 GHz detection structure, with pixel-size and 20 dB signal separation requirements, has been revealed feasible. It implies rigorous modeling of the superconducting

transmission lines, and the method proposed in this paper could be applied to other structures for similar applications.

REFERENCES

1. Nati, F., et al., "The OLIMPO experiment," *New Astronomy Reviews*, Vol. 51, 385–389, 2007.
2. Kuo, J. and E. Shih, "Microstrip stepped-impedance resonator bandpass filter with an extended optimal rejection bandwidth," *IEEE Trans. MTT*, Vol. 51, No. 5, 1554–1559, May 2003.
3. Meyers, M. J., et al., "An antenna-coupled bolometer with an integrated microstrip bandpass filter," *APL 86*, 114103, 2005.
4. Knorr, J. B., "Slot line transition," *IEEE Trans. MTT*, Vol. 22, No. 5, 548–554, May 1974.
5. Febvre, P., C. Boutez, S. George, and G. Beaudin, "Models of superconducting microstrip and coplanar elements for submillimeter applications," *Proc. of the Int. Conf. on Millimeter and Submillimeter Waves and Applications II*, Vol. SPIE 2558, 136–147, San Diego Convention Center, July 9–14, 1995.
6. Mattis, D. C. and J. Bardeen, "Theory of anomalous skin effect," *Phys. Rev.*, Vol. 111, No. 2, 412–417, 1958.